

University of Mississippi

eGrove

Faculty and Student Publications

Pharmacy, School of

7-1-2021

Assessment of evolutionary relationships for prioritization of myxobacteria for natural product discovery

Andrew Ahearne

University of Mississippi School of Pharmacy

Hanan Albataineh

University of Mississippi School of Pharmacy

Scot E. Dowd

MR DNA

D. Cole Stevens

University of Mississippi School of Pharmacy

Follow this and additional works at: https://egrove.olemiss.edu/pharmacy_facpubs



Part of the [Pharmacy and Pharmaceutical Sciences Commons](#)

Recommended Citation

Ahearne, A.; Albataineh, H.; Dowd, S.E.; Stevens, D.C. Assessment of Evolutionary Relationships for Prioritization of Myxobacteria for Natural Product Discovery. *Microorganisms* 2021, 9, 1376. <https://doi.org/10.3390/microorganisms9071376>

This Article is brought to you for free and open access by the Pharmacy, School of at eGrove. It has been accepted for inclusion in Faculty and Student Publications by an authorized administrator of eGrove. For more information, please contact egrove@olemiss.edu.



Communication

Assessment of Evolutionary Relationships for Prioritization of Myxobacteria for Natural Product Discovery

Andrew Ahearne ^{1,†}, Hanan Albatineh ^{1,†}, Scot E. Dowd ² and D. Cole Stevens ^{1,*}

¹ Department of BioMolecular Sciences, School of Pharmacy, University of Mississippi, Oxford, MS 38677, USA; aahearne@go.olemiss.edu (A.A.); haalbata@go.olemiss.edu (H.A.)

² MR DNA, Molecular Research LP, Shallowater, TX 79363, USA; sdowd@mrndnlab.com

* Correspondence: stevens@olemiss.edu; Tel.: +1-662-915-5730

† These authors contributed equally to this work.

Abstract: Discoveries of novel myxobacteria have started to unveil the potentially vast phylogenetic diversity within the family Myxococcaceae and have brought about an updated approach to myxobacterial classification. While traditional approaches focused on morphology, 16S gene sequences, and biochemistry, modern methods including comparative genomics have provided a more thorough assessment of myxobacterial taxonomy. Herein, we utilize long-read genome sequencing for two myxobacteria previously classified as *Archangium primigenium* and *Chondrocooccus macrosporus*, as well as four environmental myxobacteria newly isolated for this study. Average nucleotide identity and digital DNA–DNA hybridization scores from comparative genomics suggest previously classified as *A. primigenium* to instead be a novel member of the genus *Melittangium*, *C. macrosporus* to be a potentially novel member of the genus *Corallocooccus* with high similarity to *Corallocooccus exercitus*, and the four isolated myxobacteria to include another novel *Corallocooccus* species, a novel *Pyxidicooccus* species, a strain of *Corallocooccus exiguus*, and a potentially novel *Myxococcus* species with high similarity to *Myxococcus stipitatus*. We assess the biosynthetic potential of each sequenced myxobacterium and suggest that genus-level conservation of biosynthetic pathways support our preliminary taxonomic assignment. Altogether, we suggest that long-read genome sequencing benefits the classification of myxobacteria and improves determination of biosynthetic potential for prioritization of natural product discovery.

Keywords: myxobacteria; *Myxococcus* sp.; *Corallocooccus* sp.; *Melittangium* sp.; *Archangium* sp.; biosynthetic gene clusters



Citation: Ahearne, A.; Albatineh, H.; Dowd, S.E.; Stevens, D.C. Assessment of Evolutionary Relationships for Prioritization of Myxobacteria for Natural Product Discovery. *Microorganisms* **2021**, *9*, 1376. <https://doi.org/10.3390/microorganisms9071376>

Academic Editors: David Whitworth and Ulrich Stingl

Received: 31 March 2021

Accepted: 21 June 2021

Published: 24 June 2021

Publisher's Note: MDPI stays neutral with regard to jurisdictional claims in published maps and institutional affiliations.



Copyright: © 2021 by the authors. Licensee MDPI, Basel, Switzerland. This article is an open access article distributed under the terms and conditions of the Creative Commons Attribution (CC BY) license (<https://creativecommons.org/licenses/by/4.0/>).

1. Introduction

Over the last decade, 34 novel species of myxobacteria have been described including representatives from 10 newly described genera within the order *Myxococcales* (Table S1) [1–14]. Prevalent in soils and marine sediments, predatory and cellulolytic myxobacteria contribute to nutrient cycling within microbial food webs. Perhaps most-studied for their cooperative lifestyles, myxobacteria have been an excellent resource for investigations concerning developmental multicellularity and two-component signaling, swarming motilities and predatory features, and the discovery of biologically active metabolites [15–23]. Each of these areas of interest have benefited from the increased utility and accessibility of next-generation sequencing (NGS) technologies. The driving force behind the recent surge in efforts to discover novel species of myxobacteria can also be attributed to advances in sequencing technologies. Genome sequencing of myxobacteria has demonstrated that they possess large genomes replete with biosynthetic gene clusters, and myxobacteria have recently been deemed a “gifted” taxon for the production of specialized metabolites with drug-like properties [24–29]. These efforts, combined with a thorough metabolic survey of over 2000 strains within the order *Myxococcales*, concluded that the odds of novel metabolite discovery increase when exploring

novel genera of myxobacteria [30]. Motivated by these observations, we sought to isolate novel myxobacteria from lesser-studied North American soils.

Recently, comparative genomic analyses have been utilized to provide efficient preliminary classification of novel myxobacteria, and we considered that such an approach would expedite prioritization of strains for future metabolic studies [3,8,11,31–37]. While traditional myxobacterial classification efforts relied on morphology, biochemistry, and the conservation of 16S gene sequences, updated methods including genome-based taxonomy have provided excellent preliminary taxonomic classification of myxobacterial isolates [38–40]. Considering that genome sequencing would also afford the biosynthetic potential of any isolated myxobacteria, we sought to employ long-read sequencing to generate high-quality draft genomes hoping to avoid fragmented, partial biosynthetic pathways. For example, of the 11 currently sequenced myxobacteria from the genus *Coralloccoccus*, 68% of the 621 total putative biosynthetic gene clusters (BGCs) predicted by the analysis platform AntiSMASH are positioned on a contig edge and are potentially incomplete (Table S2). In fact, the only two *Coralloccoccus* genomes sequenced with long-read techniques (*Coralloccoccus coralloides* DSM 2259^T and *C. coralloides* strain B035) each included 34 predicted BGCs with none located on a contig edge [41,42]. Ideally, larger contigs generated from long-read sequencing might benefit the comparative genomic analyses and provide a more complete assessment of biosynthetic potential.

In addition to four environmental isolates of putative myxobacteria included in this study, we acquired two previously characterized myxobacteria from the American Type Culture Collection (ATCC): *Archangium primigenium* ATCC 29,037 and *Chondroccoccus macrosporus* ATCC 29039. Previously miscategorized as *Polyangium primigenium*, the original morphological descriptions for *A. primigenium* were remarkably apt for the strain acquired from the ATCC and cultivated in our lab, including obvious fruiting body formation and carotene-like pigmentation (Figure 1) [43,44]. The original description of *A. primigenium* fruiting bodies initially piqued our interest in the strain as members of the genus *Archangium* typically do not or very rarely form defined fruiting bodies when cultivated with standard laboratory conditions [45,46]. *Archangium* species have previously been referred to as “degenerate forms” of myxobacteria due to diminished fruiting bodies with no sporangioles or absent fruiting body formation [46]. Comparatively, little historical data is available for *C. macrosporus* ATCC 29039. The strain was deposited at the ATCC by distinguished taxonomist Professor V. B. D. Skerman and was subsequently included in a methodology study focused on isolating myxobacteria from soils [47–49]. The decision to change the genus *Chondroccoccus* to instead be *Coralloccoccus* has been validated with many novel *Coralloccoccus* species being described afterwards [8,40,50]. However, we were curious to determine the status of *C. macrosporus* ATCC 29039. Considering the proposed reassignment of *Coralloccoccus macrosporus* DSM 14697^T to the genus *Myxococcus*, it was unclear if *C. macrosporus* ATCC 29,039 should also be reassigned. Both characterized using traditional approaches that heavily relied on morphology, we sought to determine how genomic comparisons might impact the current taxonomic assignments of these available myxobacteria.

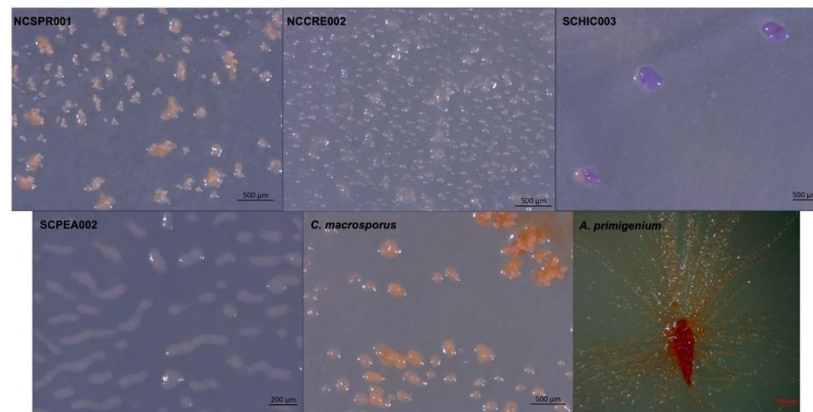


Figure 1. Myxobacterial fruiting bodies from strains NCSPR001, NCCRE002, SCHIC003, SCPEA002, and the strains *C. macrosporus* ATCC 29,039 and *A. primigenium* ATCC 29037.

2. Materials and Methods

2.1. Bacterial Strains and Growth Conditions

A. primigenium and *C. macrosporus* were procured from the ATCC as strain numbers ATCC 29037 and ATCC 29039, respectively. The remaining strains were isolated from soil as described later. All strains were cultured either on VY/2 or VY/4 agar plates (5 or 2.5 g/L baker's yeast, 1.5 g/L $\text{CaCl}_2 \cdot 2\text{H}_2\text{O}$, 0.5 mg/L vitamin B12, 15 g/L agar, pH 7.2). Swarming and fruiting bodies on agar plates were observed under a Zeiss discovery V12 stereo microscope and photographed using a Zeiss axiocam105.

2.2. Isolation of Environmental Myxobacteria

Soil samples, collected in Asheville, NC and Tryon, SC, were taken from the base of trees and dried in open air before storage. Detailed location data are provided as Supplemental Information (Table S3). Myxobacteria were isolated using a slightly modified Coli-spot method [51]. A 1 mg/mL solution of cycloheximide/nystatin was used to wet the soil sample to a paste-like consistency before inoculation onto an *Escherichia coli* baited WAT agar plate (1 g/L $\text{CaCl}_2 \cdot 2\text{H}_2\text{O}$, 15 g/L agar, 20 mM HEPES). To prepare the baiting plate, a lawn of *E. coli* was grown overnight on tryptone soya broth (TSB) with agar (1.5%), and the cells were scraped and suspended in 2 mL of sterile deionized water. Four hundred μL of the *E. coli* suspension was spread over the surface of a WAT agar plate to create a bait circle of approximately 2 inches in diameter and let dry. Once the *E. coli* was dried, a pea sized amount of soil paste was placed at the center of the bait circle. Plates were incubated at 25 °C for up to a month, and degradation of the *E. coli* was monitored over time. Visible degrading swarms were seen after a few days, and swarm edges or fruiting bodies were passaged onto VY/4 media for purification. Purification was accomplished by repeated swarm edge transfer.

2.3. Genomic DNA Isolation, Sequencing, Assembly, and Annotation

Genomic DNA for NGS was obtained from actively growing bacteria on VY/2 or VY/4 plates using NucleoBond high molecular weight DNA kit (Macherey-Nagel, Bethlehem, PA, USA). The quantity and quality of the extraction were checked by Nanodrop (Thermo Scientific NanoDrop One) and followed by Qubit quantification using Qubit[®] dsDNA HS Assay Kit (ThermoFisher Scientific, Suwanee, GA, USA).

Sequencing for all samples was performed on a Pacific Biosciences single-molecule real-time (SMRT) sequencing platform at the MR DNA facility (Shallowater, TX, USA). The SMRTbell libraries for the sample were prepared using the SMRTbell Express Template Prep Kit 2.0 (Pacific Biosciences, Menlo Park, CA, USA) following the manufacturer's user guide. Following library preparation, the final concentration of each library was measured using the Qubit[®] dsDNA HS Assay Kit (ThermoFisher Scientific, Suwanee, GA, USA), and the average library sizes were determined using the Agilent 2100 Bioanalyzer

(Agilent Technologies, Santa Clara, CA, USA). Each library pool was then sequenced using the 10-h movie time on the PacBio Sequel (Pacific Biosciences, Menlo Park, CA, USA). De Novo Assembly of each genome was accomplished using the PacBio SMRT Analysis Hierarchical Genome Assembly Process (HGAP). Genome annotation was done using Rapid Annotation using Subsystem Technology (RAST) with further annotation requested by the NCBI Prokaryotic Genome Annotation Pipeline [52]. Sequencing data have been deposited in NCBI under the accession numbers JADWYI000000000.1, JAFIMU000000000, JAFIMS000000000, JAFIMT000000000, CP071090, and CP071091 for strains *A. primigenium*, *C. macrosporus*, NCSPR001, NCCRE002, SCPEA002, and SCHIC003, respectively.

2.4. Comparative Genomic Studies

The genome sequence data were uploaded to the Type (Strain) Genome Server (TYGS), a free bioinformatics platform available under <https://tygs.dsmz.de> (accessed 10 January 2021), for a whole genome-based taxonomic analysis. TYGS was used to calculate the dDDH values and construct minimum evolution trees using the Genome BLAST Distance Phylogeny approach (GBDP) [53,54]. GBDP trees were visualized using MEGA-X [55]. The average nucleotide identity (ANI) was calculated using the ANI/AAI-Matrix calculator [56,57].

2.5. BiG-SCAPE Analysis

Genome data for all myxobacteria belonging to the *Cystobacterineae* suborder were downloaded from the NCBI database. A list of all myxobacteria used in this analysis are listed in List S1. These genomes in addition to genomes of *A. primigenium*, *C. macrosporus*, and the environmental isolates were analyzed by the AntiSMASH platform (version 5 available at <https://docs.antismash.secondarymetabolites.org>; accessed 1 February 2021) to assess specialized metabolite gene clusters using the “relaxed” strictness setting [58,59]. A total of 1826 predicted BGCs (.gbk files) were then processed locally using the BiG-SCAPE program (version 20181005, available at <https://git.wageningenur.nl/medema-group/BiG-SCAPE>; accessed 1 February 2021), with the MiBIG database (version 2.0 available at <https://mibig.secondarymetabolites.org>; accessed 1 February 2021) as reference [60,61]. BiG-SCAPE analysis was supplemented with Pfam database version 33.1 [62]. The singleton parameter in BiG-SCAPE was selected to ensure that BGCs with distances lower than the default cutoff distance of 0.3 were included in the corresponding output data. The hybrids-off parameter was selected to prevent hybrid BGC redundancy. Generated network files separated by BiG-SCAPE class were combined for visualization using Cytoscape version 3.8.2 (<http://www.cytoscape.org>; accessed 1 February 2021) [63]. Annotations associated with each BGC were included in Cytoscape networks by importing curated tables generated by BiG-SCAPE.

3. Results

3.1. Comparative Genomics and Taxonomic Assessment of *Archangium Primigenium*, *Chondrococcus Macrosporus*, and Environmental Isolates

Genome sequencing provided high quality draft genomes for each of the six investigated myxobacteria, as indicated by the summary of general features in Table 1. The total genome sizes ranged from ~9.5–13 Mb, and the %GC content varied around ~69–71%. Of the six genomes, both environmental strains SCHIC003 and SCPEA002 were assembled on a single contig. Overall, the assemblies for each genome provided much lower total contig counts (1–17) than recently sequenced myxobacterial genomes [3,8]. Interestingly, a minimum evolution of phylogenetic trees generated from the whole genome sequence data clustered *A. primigenium* with *Melittangium boletus* DSM 14713^T and not with the three currently sequenced strains from the genus *Archangium* (Figure 2, Figures S1 and S2). Accordingly, ANI and dDDH values supported the placement of *A. primigenium* in the genus *Melittangium* (Table 2) as a novel species with both values well below the established cutoffs for classification of distinct species (<95% ANI; <70% dDDH) [31,34,35,37,64]. These data suggest *A. primigenium* is currently misclassified as a member of the genus *Archangium* and should instead be placed in the genus *Melittangium*.

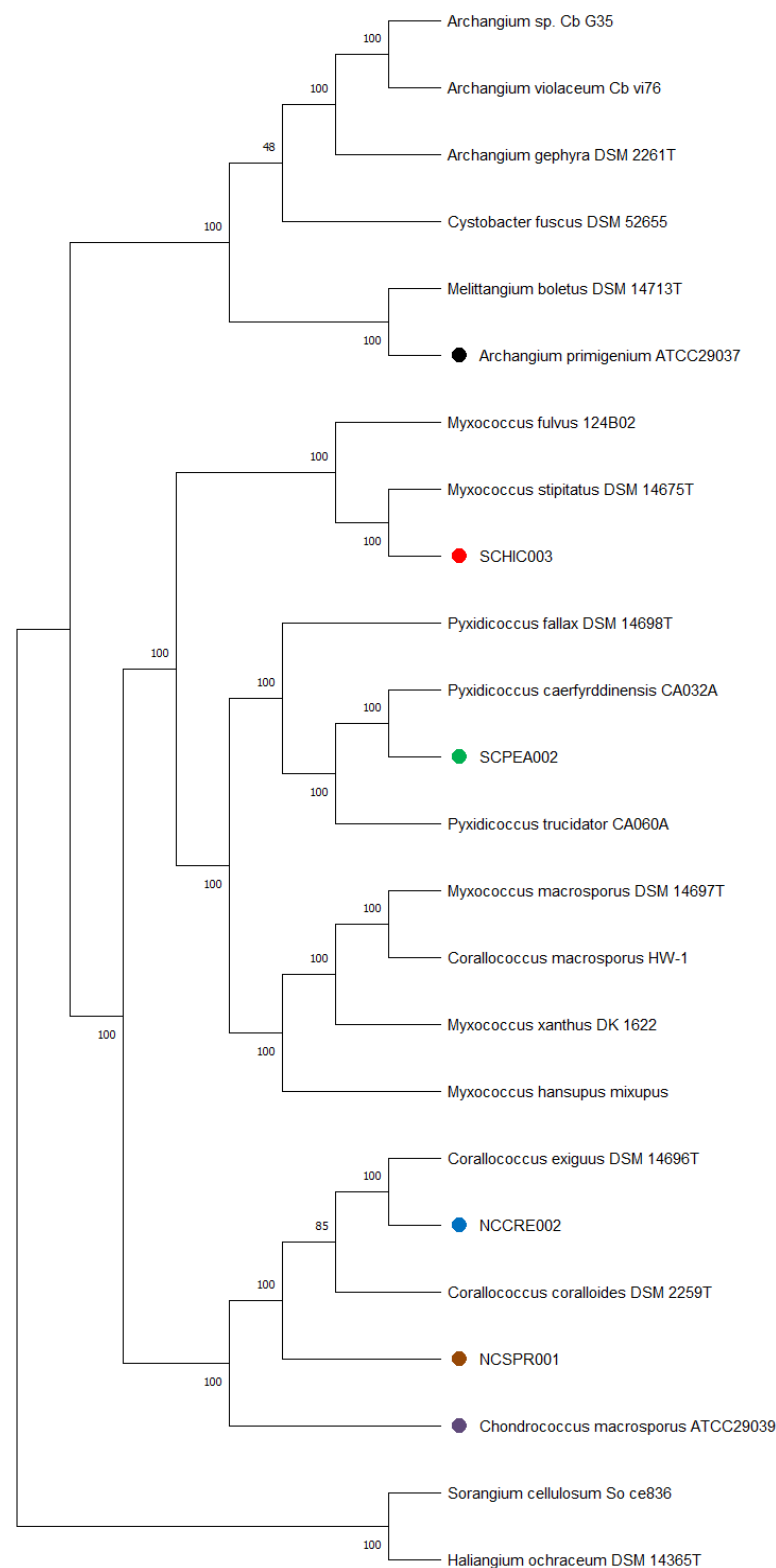


Figure 2. Minimum evolution tree from the whole genomes of different myxobacteria including the six strains under investigation in this study using the GBDP approach. The numbers in bold above branches are GBDP pseudo-bootstrap support values > 60% from 100 replications, with an average branch support of 100.0%. Branch pseudo-bootstraps less than 50% are not shown. The numbers below branches are branch lengths scaled in terms of GBDP distance formula d_5 . The tree was rooted at the midpoint.

Table 1. Genome properties and general features of myxobacteria under investigation in this study.

Species	Size (bp)	CDS	GC%	N50	L50	Contigs	Coverage
<i>A. primigenium</i>	9,491,554	7873	70.7%	9,468,833	1	3	441x
<i>C. macrosporus</i>	9,811,739	7977	70.4%	1,094,727	2	17	300x
NCSPR001	9,785,177	8033	70.1%	9,343,940	1	3	312x
NCCRE002	10,538,407	8589	69.7%	3,024,381	2	8	479x
SCPEA002	13,211,253	10,588	69.6%	N/A	1	1	144x
SCHIC003	10,367,529	8339	68.6%	N/A	1	1	301x

Table 2. 16S rRNA identity, ANI, and dDDH values for pairwise comparisons between *A. primigenium* with the most similar fully sequenced myxobacteria.

Species	16s rRNA	dDDH	ANI
<i>M. boletus</i> DSM 14713 ^T	98.89%	29.5	86.1%
<i>C. fuscus</i> DSM 52655	98.7%	24.5	83.29%
<i>A. gephyra</i> DSM 2261 ^T	97.72%	23.2	81.41%
<i>S. aurantiaca</i> DW43-1	96.06%	20	78.9%
<i>M. macrosporus</i> DSM 14697 ^T	96.63%	19.8	78.85%

The calculated ANI and dDDH values for the sequenced *C. macrosporus* strain acquired from the ATCC support the original assignment to the genus *Chondrocooccus*, now *Corallocooccus* [31,50]. As opposed to the recently reclassified *Myxococcus macrosporus* DSM 14697^T, previously *Corallocooccus macrosporus*, the minimum evolution phylogenetic tree suggested *C. macrosporus* ATCC 29039 to be a member of the genus *Corallocooccus* most similar to *Corallocooccus exercitus* DSM 108849^T (Figure 2, Figures S1 and S3) [50]. The isolated strains NCCRE002 and NCSPR001 were also determined to be members of the genus *Corallocooccus* (Figure 2, Figures S1 and S3). Comparative genome analyses implied that strain NCCRE002 is an isolate of *Corallocooccus exiguus* DSM 14696^T. However, the ANI and GBDP trees suggested that strain NCSPR001 is a novel member of the genus *Corallocooccus* most similar to *Corallocooccus coralloides* DSM 2259^T (Table 3).

The isolated SCHIC003 and SCPEA002 strains were initially determined to be members of the genus *Myxococcus*. However, inclusion of sequenced representatives from the genus *Pyxidicoccus* (considered to be synonymous with *Myxococcus*) [3] in our comparative analysis grouped strain SCPEA002 within the *Pyxidicoccus* clade (Figure 2, Figures S1 and S4). Most similar to *Pyxidicoccus caerfyrddinensis* CA032A^T, dDDH and ANI analysis suggested the SCPEA002 strain to be a novel member of the genus *Pyxidicoccus* (Table 4). Similarly, comparative genome analysis determined that strain SCHIC003 is likely be a novel member of the genus *Myxococcus*, albeit highly similar to *Myxococcus stipitatus* DSM 14675^T with ANI and dDDH values just below the cutoffs for species differentiation [31,37,64] (Table 4 and Figure 2, Figures S1 and S3).

Table 3. Differentiation chart comparing *C. macrosporus* ATCC 29039, NCCRE002, and NCSPR001 draft genome data with sequenced members of the genus *Coralloccoccus*. The top half uses total genome comparison methods (ANI and dDDH) while the bottom half uses 16S rRNA sequence for pairwise comparison. Orange shading represents species that would be designated as the same using the designated method. Blue shading represents unique species using the designated method, <98.65% 16S identity%, or < 95%/70% for ANI/dDDH.

	NCCRE002	NCSPR001	<i>Chondroccoccus macrosporus</i>	<i>Coralloccoccus interemptor</i> T	<i>Coralloccoccus terminator</i> T	<i>Coralloccoccus sicarius</i> T	<i>Coralloccoccus praedator</i> T	<i>Coralloccoccus macrosporus</i> HW1	<i>Coralloccoccus llansteffanensis</i> T	<i>Coralloccoccus exiguus</i> T	<i>Coralloccoccus exercitus</i> T	<i>Coralloccoccus coralloides</i> T	<i>Coralloccoccus carmarthenensis</i> T	<i>Coralloccoccus aberystwythensis</i> T	<i>Coralloccoccus</i> Z5C101001	<i>Coralloccoccus</i> ZKHCC1_1396	<i>Coralloccoccus</i> CA053C
NCCRE002	100%	dDDH: 51 ANI: 94	41	44	29	29	30	21	30	66	43	54	43	43	34	29	30
NCSPR001	99.8	100%	91 dDDH: 41 ANI: 91	92	86	86	86	81	87	96	91	94	92	91	88	86	86
<i>Chondroccoccus macrosporus</i>	99.15	99.22	100%	dDDH: 42 ANI: 91	30	30	30	21	31	41	51	42	43	44	34	30	31
<i>Coralloccoccus interemptor</i> T	99.8	99.87	99.35	100%	dDDH: 29 ANI: 86	30	30	21	30	44	42	46	42	42	34	30	30
<i>Coralloccoccus terminator</i> T	99.03	98.96	99.09	98.96	100%	dDDH: 35 ANI: 89	49	21	35	29	30	29	30	30	31	42	34
<i>Coralloccoccus sicarius</i> T	98.89	98.83	98.98	98.83	99.61	100%	dDDH: 35 ANI: 89	81	89	86	87	86	87	87	87	91	89
<i>Coralloccoccus praedator</i> T	99.03	98.96	99.09	98.96	100	99.61	100%	dDDH: 21 ANI: 81	36	30	31	30	31	31	32	43	35
<i>Coralloccoccus macrosporus</i> HW1	97.73	97.66	98.37	97.79	97.72	97.72	97.72	100%	dDDH: 22 ANI: 81	21	21	21	21	21	21	21	21
<i>Coralloccoccus llansteffanensis</i> T	98.83	98.76	98.89	98.76	99.54	99.93	99.54	97.73	100%	dDDH: 30 ANI: 87	32	31	32	31	33	36	54
<i>Coralloccoccus exiguus</i> T	99.93	99.87	99.22	99.87	99.09	98.96	99.09	97.79	98.89	100%	dDDH: 43 ANI: 91	88	87	87	88	89	94
<i>Coralloccoccus exercitus</i> T	99.02	99.09	99.87	99.22	99.22	99.09	99.22	98.37	99.02	99.09	100%	dDDH: 44 ANI: 92	54	44	34	30	30
<i>Coralloccoccus coralloides</i> T	99.67	99.61	99.09	99.74	98.83	98.7	98.83	97.66	98.63	99.74	98.96	100%	dDDH: 44 ANI: 92	48	34	30	30
<i>Coralloccoccus carmarthenensis</i> T	99.22	99.28	99.93	99.28	99.15	99.02	99.15	98.31	98.96	99.28	99.8	99.02	100%	dDDH: 48 ANI: 93	88	87	87
<i>Coralloccoccus aberystwythensis</i> T	99.35	99.15	99.8	99.15	99.15	99.02	99.15	98.31	98.96	99.26	99.67	99.02	99.87	100%	dDDH: 35 ANI: 89	31	31
<i>Coralloccoccus</i> Z5C101001	98.76	98.83	99.48	98.83	99.22	99.22	99.22	98.11	99.15	98.83	99.61	98.57	99.54	99.41	100%	dDDH: 32 ANI: 88	32
<i>Coralloccoccus</i> ZKHCC1_1396	98.7	98.89	98.89	98.76	99.67	99.35	99.67	97.4	99.28	98.76	99.02	98.5	98.96	98.83	99.09	100%	dDDH: 35 ANI: 88
<i>Coralloccoccus</i> CA053C	98.57	98.5	98.7	98.5	99.54	99.67	99.54	97.59	99.61	98.63	98.83	98.37	98.76	98.76	99.22	99.28	100%

Table 4. Differentiation chart comparing SCPEA002 and SCHIC003 draft genome data with sequenced members of the genera *Myxococcus* and *Pyxidicoccus*. The top half uses total genome comparison methods (ANI and dDDH) while the bottom half uses 16S rRNA sequence for pairwise comparison. Orange shading represents species that would be designated as the same using the designated method. Blue shading represents unique species using the designated method, <98.65% 16S identity%, or < 95%/70% for ANI/dDDH.

	SCPEA002	SCHIC003	<i>M. fulvus</i> 124B02	<i>P. fallax</i> T	<i>M. stipitatus</i> T	<i>M. hansupus</i>	<i>M. eversor</i> T	<i>M. llanfair</i> T	<i>M. vastator</i> T	<i>M. virescens</i> T	<i>P. truncidator</i> T	<i>P. caerfyrdi-</i> <i>nensis</i> T	<i>M. xanthus</i> DK1622	<i>M. macrosporus</i> T
SCPEA002	100%	dDDH: 22 ANI: 82	23 82	28 85	22 82	23 83	23 82	28 82	25 83	24 83	29 86	34 88	24 83	24 83
SCHIC003	99.15%	100%	dDDH: 26 ANI: 84	23 82	49 93	22 81	27 85	27 85	23 82	22 82	22 82	22 82	22 81	22 82
<i>M. fulvus</i> 124B02	99.61%	99.41%	100%	dDDH: 23 ANI: 82	26 84	22 82	28 85	28 85	23 82	23 82	23 82	23 82	22 82	23 82
<i>P. fallax</i> T	99.54%	98.96%	99.41%	100%	dDDH: 23 ANI: 82	24 83	23 82	23 82	25 84	25 83	30 86	29 86	25 83	25 84
<i>M. stipitatus</i> T	99.15%	100%	99.41%	98.96%	100%	dDDH: 22 ANI: 81	27 85	27 85	23 82	22 82	22 82	22 82	29 81	22 82
<i>M. hansupus</i>	98.89%	98.44%	98.89%	98.57%	98.44%	100%	dDDH: 22 ANI: 82	23 82	32 88	32 87	24 83	24 83	31 87	32 88
<i>M. eversor</i> T	98.83%	98.24%	98.83%	98.50%	98.24%	99.15%	100%	dDDH: 41 ANI: 91	23 82	22 82	24 82	23 82	22 82	23 82
<i>M. llanfair</i> T	98.76%	98.31%	98.89%	98.44%	98.31%	99.09%	99.93%	100%	dDDH: 23 ANI: 82	23 82	24 83	23 82	23 82	23 82
<i>M. vastator</i> T	98.70%	98.24%	98.70%	98.37%	98.24%	99.41%	98.96%	98.89%	100%	dDDH: 52 ANI: 94	25 84	25 84	52 94	41 91
<i>M. virescens</i> T	98.63%	98.14%	98.63%	98.31%	98.18%	99.35%	98.89%	98.83%	99.67%	100%	dDDH: 25 ANI: 83	24 83	73 97	40 90
<i>P. truncidator</i> T	99.09%	98.37%	98.70%	99.02%	98.37%	98.89%	98.83%	98.76%	98.70%	98.63%	100%	dDDH: 33 ANI: 88	24 83	25 84
<i>P. caerfyrdinensis</i> T	99.48%	98.76%	99.09%	99.41%	98.76%	99.15%	98.96%	98.89%	98.96%	98.96%	99.61%	100%	dDDH: 24 ANI: 83	25 83
<i>M. xanthus</i> DK1622	98.57%	98.11%	98.57%	98.24%	98.11%	99.28%	98.83%	98.76%	99.74%	99.93%	98.57%	98.83%	100%	dDDH: 40 ANI: 90
<i>M. macrosporus</i> T	98.89%	98.44%	98.89%	98.57%	98.44%	99.48%	99.15%	99.09%	99.67%	99.61%	98.89%	99.15%	99.54%	100%

3.2. Biosynthetic Potential and Genus Level Correlations

Analysis of our draft genomes using the biosynthetic pathway prediction platform AntiSMASH revealed a range of 29–42 total predicted BGCs with *C. macrosporus* including the highest total of BGCs. However, the draft genome for *C. macrosporus* also included the highest total of four partial BGCs positioned on the edges of contigs. No BGCs occurring on contig edges were observed from *A. primigenium*, NCSPR001, or SCPEA002. All of the sequenced strains included highly similar ($\geq 75\%$ similarity score) biosynthetic pathways for the signaling terpene geosmin [65,66], the signaling lipids VEPE/AEPE/TG-1 [67,68], and carotenoids [69–72] (Figure 3). Excluding SCHIC003, each genome included a BGC highly homologous to the pathway associated with the myxobacterial siderophore myxochelin [73,74]. Pathways somewhat similar (similarity scores of 66%) to the myxoprincomide-c506 BGC were observed in every genome except the *A. primigenium* genome [75]. Clusters with $\geq 75\%$ similarity to pathways from *M. stipitatus* DSM 14675^T associated with the metabolites rhizopodin [76,77] and phenalamide A2 [78] were observed in the SCHIC003 draft genome as well as clusters also present in the *M. stipitatus* DSM 14675^T genome deposited in the AntiSMASH database [79], including the dkxanthene [80], fulvuthiacene [81], and violacein [82–84] BGCs (Figure 4). Considering previously characterized BGCs from each genus associated with the six investigated myxobacteria, the coralolopyronin BGC from *C. coralloides* B035 [85,86] was absent from all three of the putative *Corallocooccus* strains, the melithiazol BGC from *Melittangium lichenicola* Me I46 [87] was not present in *A. primigenium*, and neither the disciformycin/gulmirecin BGC [88,89] or the pyxidicycline BGC [90] from *Pyxidicoccus fallax* were present in SCPEA002.

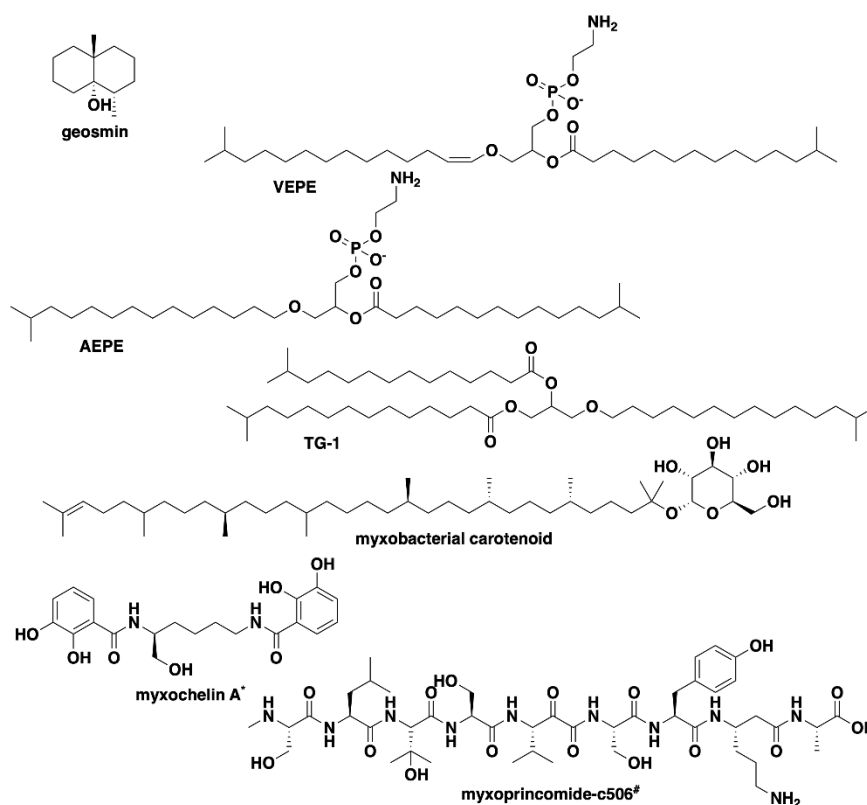


Figure 3. Common specialized metabolites from myxobacteria associated with characterized BGCs present in the six investigated strains of myxobacteria. * Myxochelin BGC not present in SCHIC003 genome data. # Myxoprincomide BGC not present in *A. primigenium* genome data.

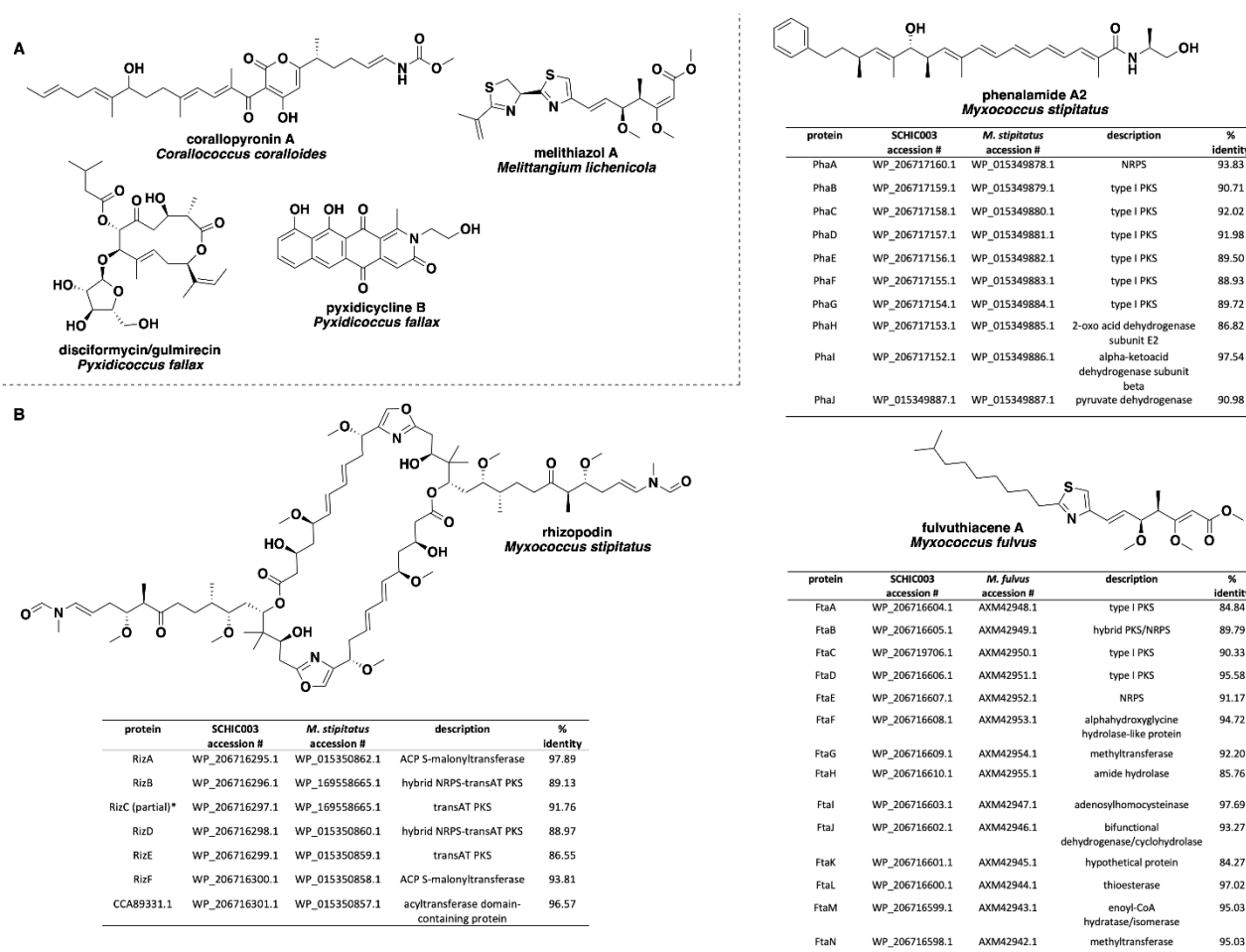


Figure 4. (A) Specialized metabolites produced by members of the genera *Corallocooccus*, *Melittangium*, and *Pyxidicoccus* with no associated BGCs observed in any of the six investigated myxobacterial strains. (B) Comparisons of the rhizopodin, phenalamide A2, and fulvuthiacene BGCs from SCHIC003 genome data and the characterized pathways from *M. stipitatus* and *M. fulvus*. All SCHIC003 gene products, excluding RizC, had coverages $\geq 99\%$ with the indicated homolog. * RizC located on a contig edge and is incomplete in SCHIC003 genome data.

Utilizing the BiG-SCAPE platform to render BGC sequence similarity networks, we sought to determine the extent of homology between BGCs from our six sequenced myxobacteria and BGCs from all currently sequenced members of the suborder *Cystobacterineae* [91]. The resulting sequence similarity network included 1080 BGCs connected by 3046 edges (not including self-looped nodes/singletons) and depicted genus-level homologies across all BGCs from the newly sequenced myxobacteria corroborating our suggested taxonomic assignments (Figure 5 and Table 5). For example, BGCs from the three newly sequenced samples *C. macrosporus*, NCSRP001, and NCCRE002 were almost exclusively clustered with BGCs from members of the genus *Corallocooccus*, and BGCs from SCHIC003 and SCPEA002 samples clustered with the genera *Myxococcus* and *Pyxidicoccus* (Figure 5). However, SCPEA002 BGCs do not cluster as frequently with *Pyxidicoccus* BGCs as they do *Myxococcus* BGCs, and the majority (76.5%) were not clustered with any BGC within the network (Table 5). This is likely due to the highly fragmented nature of available *Pyxidicoccus* genomes resulting in many incomplete or partial BGCs. Therefore, few *Pyxidicoccus* pathways appear in the similarity network, and the percentage of unique pathways associated with SCPEA002 is likely overestimated. Regardless, the limited number of SCPEA002 BGCs clustered with BGCs from *Myxococcus*/*Pyxidicoccus* genomes indicates a potential to discover novel metabolites despite placement in the highly scrutinized clade. The only clustered groups with numerous edges formed between BGCs from the genera

Myxococcus and *Corallocooccus* included characterized biosynthetic pathways for ubiquitous signaling lipids VEPE/AEPE/TG-1, carotenoids, and the siderophore myxochelin as well as two uncharacterized BGCs predicted to produce ribosomally synthesized and post-translationally modified peptides (RiPPs).

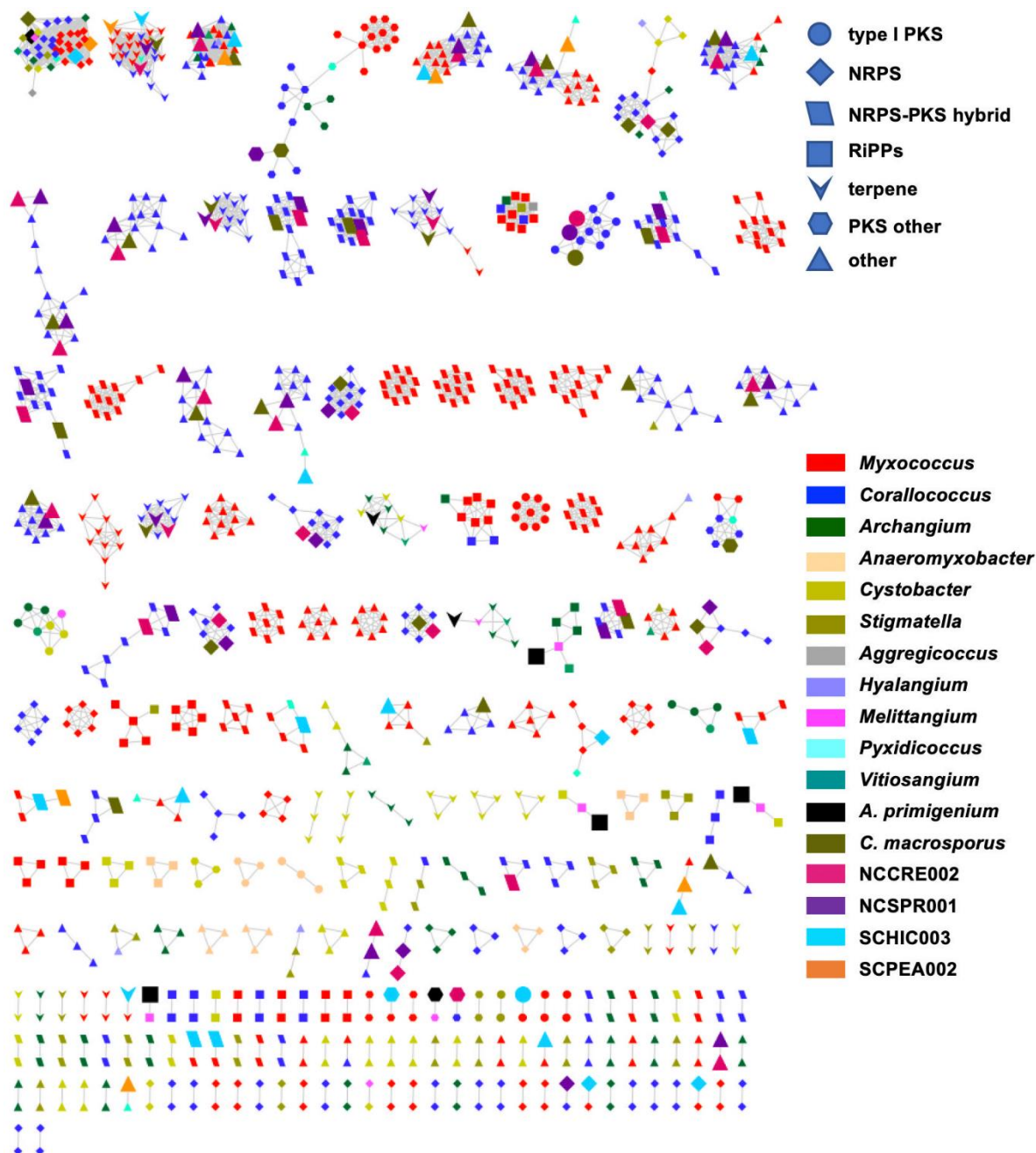


Figure 5. BiG-SCAPE BGC sequence similarity networks ($c = 0.3$) as visualized with Cytoscape. The network is generated from *A. primigenium*, *C. macrosporus*, NCCRE002, NCSPR001, SCHIC003, SCPEA002, and all myxobacteria belonging to the Cystobacterineae suborder with genomes deposited in NCBI. Each node represents one BGC identified by AntiSMASH 5.0, where the colors and shapes of the nodes represent different genera and AntiSMASH-predicted classes, respectively. Nodes representing BGCs from newly sequenced myxobacteria included in this study are enlarged. BGCs included as singletons in the original BiG-SCAPE analysis removed.

Table 5. Overview of BiG-SCAPE BGC sequence similarity networks of the six strains under investigation in this study.

Myxobacteria	# of Total BGCs	# and % of Singletons	# of Edges Formed with other BGCs	# of BGCs with 1 or 2 Edges	# of BGCs with 3 or More Edges
<i>A. primigenium</i> ATCC 29037	32	24 (75%)	21	6	2
<i>C. macrosporus</i> ATCC 29039 *	42	9 (21.4%)	228	4	29
NCSPR001	32	1 (3.1%)	248	7	24
NCCRE002 *	36	3 (16.7%)	231	7	26
SCPEA002	34	26 (76.5%)	62	4	4
SCHIC003	29	8 (27.6%)	85	13	8

* genomes with fragmented biosynthetic pathways, likely resulting in fewer clustered pathways than truly exist.

Interestingly, a total of 23 *A. primigenium* BGCs (out of 32 BGCs) appear as singletons in the network with no homology to any of the included BGCs from *Cystobacterineae*. In fact, aside from the VEPE/AEPE/TG-1 cluster and a terpene cluster that included members of the genera *Archangium* and *Cystobacter*, all remaining BGCs from *A. primigenium* had connecting edges to BGCs from *Melittangium boletus* DSM 14713^T. Out of 21 edges formed by *A. primigenium* in the network, four edges were formed with four species of *Corallocooccus* (a total of 11 *Corallocooccus* species in the network), four edges were formed with all species of *Cystobacter* (three species in the network), six edges were formed with all species of *Archangium* (three species in the network), and seven edges were formed with the only *Melittangium* species in the network, *M. boletus* DSM 14713^T. Overall, these data corroborate our preliminary taxonomic assignments and suggest that the prioritization of *A. primigenium* for subsequent discovery efforts is most likely to yield novel metabolites.

4. Discussion

As novel myxobacteria continue to be isolated and explored for natural product discovery, efficient approaches for approximate taxonomic placement will assist the prioritization of lesser studied genera. Utilizing long-read genome sequencing and comparative genomic analyses, we determine preliminary taxonomic placement for four myxobacteria isolated from North American soils and two myxobacteria deposited at the ATCC. This approach indicated that previously classified *A. primigenium* ATCC 29037 is instead a novel member of the genus *Melittangium*, and that three of our four environmental isolates included potentially novel members of the genera *Corallocooccus*, *Myxococcus*, and *Pyxidicooccus*. Previously classified *Chondrocooccus macrosporus* ATCC 29039 was also determined to be a potentially novel member of the genus *Corallocooccus*, with high similarity to *C. exercitus* DSM 108849^T and phylogenetically distinct from *M. macrosporus* DSM 14697^T previously assigned to the genus *Corallocooccus*. Subsequent bioinformatic analysis of biosynthetic pathways included in the newly sequenced genomes corroborated our preliminary taxonomic placements for each sample. Ultimately, this process identified *A. primigenium* to be a member of the lesser studied genus *Melittangium* and indicated that it should be prioritized for continued natural product discovery efforts. Of the environmental isolates, BGCs from SCPEA002 were determined to include the least amount of overlap with BGCs from other *Myxococcus/Pyxidicooccus* species. While environmental isolates SCHIC002 and NCSPR001 were also identified as novel members of the genera *Myxococcus* and *Corallocooccus*, respectively, the apparent overlap in BGCs from thoroughly explored myxobacteria determined from sequence similarity network analysis suggests a limited potential for discovery of novel specialized metabolites. Overall, comparative genomic techniques including the assessment of biosynthetic potential enabled a phylogenetic approximation and suggested prioritization of *A. primigenium* for natural product discovery efforts from a sample set of six newly sequenced myxobacteria.

Supplementary Materials: The following are available online at <https://www.mdpi.com/article/10.3390/microorganisms9071376/s1>. Supplemental Table S1: Novel myxobacteria described in

literature spanning 2011–2021; Table S2: Comparison of biosynthetic gene clusters (BGCs) located on contig edges from previously sequenced members of the genus *Coralloccoccus*, Table S3: Locations of soil samples used for environmental strains isolation, List S1: A list of all myxobacteria and their accession numbers used in BiG-SCAPE; Figure S1: Minimum evolution tree from the 16S rRNA of the 6 strains under investigation in this study and all myxobacteria Type strains deposited in DSMZ; Figure S2: Minimum evolution tree from the whole genomes of *A. primigenium* and different members of the family *Archangiaceae* using the GBDP approach; Figure S3: Minimum evolution tree from the whole genomes of *C. macrosporus* ATCC 29039, NCCRE002, NCSPR001 and different members of genus *Coralloccoccus* using the GBDP approach; Figure S4: Minimum evolution tree from the whole genomes of SCHIC003, SCPEA002, and different members of *Myxococcus* and *Pyxidicoccus* using the GBDP approach.

Author Contributions: Conceptualization, supervision, and administration D.C.S.; formal analysis and data curation A.A., H.A., S.E.D., and D.C.S.; methodology, validation, and writing A.A., H.A., and D.C.S. All authors have read and agreed to the published version of the manuscript.

Funding: This research was supported by funds from the National Institute of Allergy and Infectious Diseases (1 R15 AI137996-01A1) and the National Institute of General Medical Sciences (1 P20 GM130460-01A1).

Institutional Review Board Statement: Not applicable.

Informed Consent Statement: Not applicable.

Data Availability Statement: Sequencing data have been deposited in NCBI under the accession numbers JADWYI000000000.1, JAFIMU000000000, JAFIMS000000000, JAFIMT000000000, CP071090, and CP071091 for strains *A. primigenium*, *C. macrosporus*, NCSPR001, NCCRE002, SCPEA002, and SCHIC003, respectively.

Acknowledgments: The authors would like to acknowledge the University of Mississippi School of Pharmacy for startup support.

Conflicts of Interest: The authors declare no conflict of interest.

References

- Awal, R.P.; Garcia, R.; Gemperlein, K.; Wink, J.; Kunwar, B.; Parajuli, N.; Muller, R. *Vitiosangium cumulatum* gen. nov., sp. nov. and *Vitiosangium subalbum* sp. nov., soil myxobacteria, and emended descriptions of the genera *Archangium* and *Angiococcus*, and of the family *Cystobacteraceae*. *Int. J. Syst. Evol. Microbiol.* **2017**, *67*, 1422–1430. [[CrossRef](#)]
- Awal, R.P.; Garcia, R.; Muller, R. *Racemicystis crocea* gen. nov., sp. nov., a soil myxobacterium in the family *Polyangiaceae*. *Int. J. Syst. Evol. Microbiol.* **2016**, *66*, 2389–2395. [[CrossRef](#)]
- Chambers, J.; Sparks, N.; Sydney, N.; Livingstone, P.G.; Cookson, A.R.; Whitworth, D.E. Comparative Genomics and Pan-Genomics of the *Myxococcaceae*, including a Description of Five Novel Species: *Myxococcus eversor* sp. nov., *Myxococcus llanfairpwllgwyngyllgogerychwyrndrobwlillllyantysiliogogochensis* sp. nov., *Myxococcus vastator* sp. nov., *Pyxidicoccus caerfyrdinensis* sp. nov., and *Pyxidicoccus trucidator* sp. nov. *Genome Biol. Evol.* **2020**, *12*, 2289–2302. [[CrossRef](#)]
- Garcia, R.; Gemperlein, K.; Muller, R. *Minicystis rosea* gen. nov., sp. nov., a polyunsaturated fatty acid-rich and steroid-producing soil myxobacterium. *Int. J. Syst. Evol. Microbiol.* **2014**, *64*, 3733–3742. [[CrossRef](#)]
- Garcia, R.; Muller, R. *Simulacricoccus ruber* gen. nov., sp. nov., a microaerotolerant, non-fruiting, myxospore-forming soil myxobacterium and emended description of the family *Myxococcaceae*. *Int. J. Syst. Evol. Microbiol.* **2018**, *68*, 3101–3110. [[CrossRef](#)]
- Garcia, R.; Stadler, M.; Gemperlein, K.; Muller, R. *Aetherobacter fasciculatus* gen. nov., sp. nov. and *Aetherobacter rufus* sp. nov., novel myxobacteria with promising biotechnological applications. *Int. J. Syst. Evol. Microbiol.* **2016**, *66*, 928–938. [[CrossRef](#)] [[PubMed](#)]
- Iizuka, T.; Jojima, Y.; Hayakawa, A.; Fujii, T.; Yamanaka, S.; Fudou, R. *Pseudenygromyxa salsuginis* gen. nov., sp. nov., a myxobacterium isolated from an estuarine marsh. *Int. J. Syst. Evol. Microbiol.* **2013**, *63*, 1360–1369. [[CrossRef](#)]
- Livingstone, P.G.; Ingleby, O.; Girdwood, S.; Cookson, A.R.; Morphew, R.M.; Whitworth, D.E. Predatory Organisms with Untapped Biosynthetic Potential: Descriptions of Novel *Coralloccoccus* Species *C. aberystwythensis* sp. nov., *C. carmarthensis* sp. nov., *C. exercitus* sp. nov., *C. interemptor* sp. nov., *C. llansteffanensis* sp. nov., *C. praedator* sp. nov., *C. sicarius* sp. nov., and *C. terminator* sp. nov. *Appl. Environ. Microbiol.* **2020**, *86*. [[CrossRef](#)]
- Mohr, K.I.; Garcia, R.O.; Gerth, K.; Irschik, H.; Muller, R. *Sandaracinus amyolyticus* gen. nov., sp. nov., a starch-degrading soil myxobacterium, and description of *Sandaracinaceae* fam. nov. *Int. J. Syst. Evol. Microbiol.* **2012**, *62*, 1191–1198. [[CrossRef](#)] [[PubMed](#)]

10. Mohr, K.I.; Moradi, A.; Glaeser, S.P.; Kampfer, P.; Gemperlein, K.; Nubel, U.; Schumann, P.; Muller, R.; Wink, J. *Nannocystis konarekensis* sp. nov., a novel myxobacterium from an Iranian desert. *Int. J. Syst. Evol. Microbiol.* **2018**, *68*, 721–729. [[CrossRef](#)]
11. Mohr, K.I.; Wolf, C.; Nubel, U.; Szafranska, A.K.; Steglich, M.; Hennessen, F.; Gemperlein, K.; Kampfer, P.; Martin, K.; Muller, R.; et al. A polyphasic approach leads to seven new species of the cellulose-decomposing genus *Sorangium*, *Sorangium ambruticinum* sp. nov., *Sorangium arenae* sp. nov., *Sorangium bulgaricum* sp. nov., *Sorangium dawidii* sp. nov., *Sorangium kenyense* sp. nov., *Sorangium orientale* sp. nov. and *Sorangium reichenbachii* sp. nov. *Int. J. Syst. Evol. Microbiol.* **2018**, *68*, 3576–3586. [[CrossRef](#)] [[PubMed](#)]
12. Moradi, A.; Ebrahimipour, G.H.; Mohr, K.I.; Kampfer, P.; Glaeser, S.P.; Hennessen, F.; Gemperlein, K.; Awal, R.P.; Wolf, C.; Muller, R.; et al. *Racemicystis persica* sp. nov., a myxobacterium from soil. *Int. J. Syst. Evol. Microbiol.* **2017**, *67*, 472–478. [[CrossRef](#)]
13. Sood, S.; Awal, R.P.; Wink, J.; Mohr, K.I.; Rohde, M.; Stadler, M.; Kampfer, P.; Glaeser, S.P.; Schumann, P.; Garcia, R.; et al. *Aggregicoccus edonensis* gen. nov., sp. nov., an unusually aggregating myxobacterium isolated from a soil sample. *Int. J. Syst. Evol. Microbiol.* **2015**, *65*, 745–753. [[CrossRef](#)] [[PubMed](#)]
14. Yamamoto, E.; Muramatsu, H.; Nagai, K. *Vulгатibacter incomptus* gen. nov., sp. nov. and *Labilithrix luteola* gen. nov., sp. nov., two myxobacteria isolated from soil in Yakushima Island, and the description of *Vulгатibacteraceae* fam. nov., *Labilithrichaceae* fam. nov. and *Anaeromyxobacteraceae* fam. nov. *Int. J. Syst. Evol. Microbiol.* **2014**, *64*, 3360–3368. [[CrossRef](#)]
15. Bader, C.D.; Panter, F.; Muller, R. In depth natural product discovery—Myxobacterial strains that provided multiple secondary metabolites. *Biotechnol. Adv.* **2020**, *39*, 107480. [[CrossRef](#)] [[PubMed](#)]
16. Bretl, D.J.; Kirby, J.R. Molecular Mechanisms of Signaling in *Myxococcus xanthus* Development. *J. Mol. Biol.* **2016**, *428*, 3805–3830. [[CrossRef](#)] [[PubMed](#)]
17. Mercier, R.; Mignot, T. Regulations governing the multicellular lifestyle of *Myxococcus xanthus*. *Curr. Opin. Microbiol.* **2016**, *34*, 104–110. [[CrossRef](#)]
18. Mohr, K.I. Diversity of Myxobacteria—We Only See the Tip of the Iceberg. *Microorganisms* **2018**, *6*, 84. [[CrossRef](#)]
19. Pathak, D.T.; Wei, X.; Wall, D. Myxobacterial tools for social interactions. *Res. Microbiol.* **2012**, *163*, 579–591. [[CrossRef](#)]
20. Petters, S.; Gross, V.; Sollinger, A.; Pichler, M.; Reinhard, A.; Bengtsson, M.M.; Urich, T. The soil microbial food web revisited: Predatory myxobacteria as keystone taxa? *ISME J.* **2021**. [[CrossRef](#)]
21. Sah, G.P.; Wall, D. Kin recognition and outer membrane exchange (OME) in myxobacteria. *Curr. Opin. Microbiol.* **2020**, *56*, 81–88. [[CrossRef](#)]
22. Thiery, S.; Kaimer, C. The Predation Strategy of *Myxococcus xanthus*. *Front. Microbiol.* **2020**, *11*, 2. [[CrossRef](#)]
23. Whitworth, D.E. Genome-wide analysis of myxobacterial two-component systems: Genome relatedness and evolutionary changes. *BMC Genom.* **2015**, *16*, 780. [[CrossRef](#)]
24. Baltz, R.H. Molecular beacons to identify gifted microbes for genome mining. *J. Antibiot.* **2017**, *70*, 639–646. [[CrossRef](#)] [[PubMed](#)]
25. Baltz, R.H. Gifted microbes for genome mining and natural product discovery. *J. Ind. Microbiol. Biotechnol.* **2017**, *44*, 573–588. [[CrossRef](#)] [[PubMed](#)]
26. Herrmann, J.; Fayad, A.A.; Muller, R. Natural products from myxobacteria: Novel metabolites and bioactivities. *Nat. Prod. Rep.* **2017**, *34*, 135–160. [[CrossRef](#)] [[PubMed](#)]
27. Landwehr, W.; Wolf, C.; Wink, J. Actinobacteria and Myxobacteria—Two of the Most Important Bacterial Resources for Novel Antibiotics. *Curr. Top. Microbiol. Immunol.* **2016**, *398*, 273–302. [[CrossRef](#)] [[PubMed](#)]
28. Weissman, K.J.; Muller, R. Myxobacterial secondary metabolites: Bioactivities and modes-of-action. *Nat. Prod. Rep.* **2010**, *27*, 1276–1295. [[CrossRef](#)]
29. Wenzel, S.C.; Muller, R. Myxobacteria—‘microbial factories’ for the production of bioactive secondary metabolites. *Mol. Biosyst.* **2009**, *5*, 567–574. [[CrossRef](#)] [[PubMed](#)]
30. Hoffmann, T.; Krug, D.; Bozkurt, N.; Duddela, S.; Jansen, R.; Garcia, R.; Gerth, K.; Steinmetz, H.; Muller, R. Correlating chemical diversity with taxonomic distance for discovery of natural products in myxobacteria. *Nat. Commun.* **2018**, *9*, 803. [[CrossRef](#)]
31. Chun, J.; Oren, A.; Ventosa, A.; Christensen, H.; Arahal, D.R.; da Costa, M.S.; Rooney, A.P.; Yi, H.; Xu, X.W.; De Meyer, S.; et al. Proposed minimal standards for the use of genome data for the taxonomy of prokaryotes. *Int. J. Syst. Evol. Microbiol.* **2018**, *68*, 461–466. [[CrossRef](#)] [[PubMed](#)]
32. Chun, J.; Rainey, F.A. Integrating genomics into the taxonomy and systematics of the Bacteria and Archaea. *Int. J. Syst. Evol. Microbiol.* **2014**, *64*, 316–324. [[CrossRef](#)] [[PubMed](#)]
33. Garcia, R.; Gerth, K.; Stadler, M.; Dogma, I.J., Jr.; Muller, R. Expanded phylogeny of myxobacteria and evidence for cultivation of the ‘unculturable’. *Mol. Phylogenet. Evol.* **2010**, *57*, 878–887. [[CrossRef](#)]
34. Goris, J.; Konstantinidis, K.T.; Klappenbach, J.A.; Coenye, T.; Vandamme, P.; Tiedje, J.M. DNA-DNA hybridization values and their relationship to whole-genome sequence similarities. *Int. J. Syst. Evol. Microbiol.* **2007**, *57*, 81–91. [[CrossRef](#)]
35. Kim, M.; Oh, H.S.; Park, S.C.; Chun, J. Towards a taxonomic coherence between average nucleotide identity and 16S rRNA gene sequence similarity for species demarcation of prokaryotes. *Int. J. Syst. Evol. Microbiol.* **2014**, *64*, 346–351. [[CrossRef](#)] [[PubMed](#)]
36. Livingstone, P.G.; Morphew, R.M.; Whitworth, D.E. Genome Sequencing and Pan-Genome Analysis of 23 *Corallococcus* spp. Strains Reveal Unexpected Diversity, With Particular Plasticity of Predatory Gene Sets. *Front. Microbiol.* **2018**, *9*, 3187. [[CrossRef](#)]
37. Sangal, V.; Goodfellow, M.; Jones, A.L.; Schwalbe, E.C.; Blom, J.; Hoskisson, P.A.; Sutcliffe, I.C. Next-generation systematics: An innovative approach to resolve the structure of complex prokaryotic taxa. *Sci. Rep.* **2016**, *6*, 38392. [[CrossRef](#)]

38. Shimkets, L.; Woese, C.R. A phylogenetic analysis of the myxobacteria: Basis for their classification. *Proc. Natl. Acad. Sci. USA* **1992**, *89*, 9459–9463. [[CrossRef](#)] [[PubMed](#)]
39. Sproer, C.; Reichenbach, H.; Stackebrandt, E. The correlation between morphological and phylogenetic classification of myxobacteria. *Int. J. Syst. Evol. Microbiol.* **1999**, *49 Pt 3*, 1255–1262. [[CrossRef](#)]
40. Stackebrandt, E.; Pauker, O.; Steiner, U.; Schumann, P.; Straubler, B.; Heibei, S.; Lang, E. Taxonomic characterization of members of the genus *Coralloccoccus*: Molecular divergence versus phenotypic coherency. *Syst. Appl. Microbiol.* **2007**, *30*, 109–118. [[CrossRef](#)]
41. Bouhired, S.; Rupp, O.; Blom, J.; Schaberle, T.F.; Schiefer, A.; Kehraus, S.; Pfarr, K.; Goesmann, A.; Hoerauf, A.; König, G. Complete Genome Sequence of the Corallopyronin A-Producing Myxobacterium *Coralloccoccus coralloides* B035. *Microbiol. Resour. Announc.* **2019**, *8*, e00050-19. [[CrossRef](#)] [[PubMed](#)]
42. Huntley, S.; Zhang, Y.; Treuner-Lange, A.; Kneip, S.; Sensen, C.W.; Sogaard-Andersen, L. Complete genome sequence of the fruiting myxobacterium *Coralloccoccus coralloides* DSM 2259. *J. Bacteriol.* **2012**, *194*, 3012–3013. [[CrossRef](#)]
43. McDonald, J.C. Studies on the genus *Archangium* (Myxobacterales). II. The effect of temperature and carbohydrates on some physiological processes. *Mycologia* **1967**, *59*, 1059–1068. [[CrossRef](#)] [[PubMed](#)]
44. McDonald, J.C. Studies on the genus *Archangium* (Myxobacterales) I. Morphology. *Mycologia* **1965**, *57*, 737–747. [[CrossRef](#)]
45. Shimkets, L.J.; Dworkin, M.; Reichenbach, H. The Myxobacteria. In *The Prokaryotes*; Dworkin, M., Falkow, S., Rosenberg, E., Schleifer, K.H., Stackebrandt, E., Eds.; Springer: New York, NY, USA, 2006. [[CrossRef](#)]
46. McCurdy, H.D. Studies on the Taxonomy of the Myxobacterales. *Int. J. Syst. Bacteriol.* **1971**, *21*, 50–54. [[CrossRef](#)]
47. Starr, M.P.; Skerman, V.B. Bacterial diversity: The natural history of selected morphologically unusual bacteria. *Annu. Rev. Microbiol.* **1965**, *19*, 407–454. [[CrossRef](#)] [[PubMed](#)]
48. Sly, L.I. Taxonomic Note: V. B. D. Skerman (1921–1993), a Reforming Force in Bacterial Systematics and Nomenclature. *Int. J. Syst. Evol. Microbiol.* **1995**, *45*, 412–413. [[CrossRef](#)]
49. Karwowski, J.P.; Sunga, G.N.; Kadam, S.; McAlpine, J.B. A method for the selective isolation of *Myxococcus* directly from soil. *J. Ind. Microbiol.* **1996**, *16*, 230–236. [[CrossRef](#)]
50. Lang, E.; Stackebrandt, E. Emended descriptions of the genera *Myxococcus* and *Coralloccoccus*, typification of the species *Myxococcus stipitatus* and *Myxococcus macrosporus* and a proposal that they be represented by neotype strains. Request for an Opinion. *Int. J. Syst. Evol. Microbiol.* **2009**, *59*, 2122–2128. [[CrossRef](#)]
51. Dawid, W. Biology and global distribution of myxobacteria in soils. *FEMS Microbiol. Rev.* **2000**, *24*, 403–427. [[CrossRef](#)]
52. Aziz, R.K.; Bartels, D.; Best, A.A.; DeJongh, M.; Disz, T.; Edwards, R.A.; Formsma, K.; Gerdes, S.; Glass, E.M.; Kubal, M.; et al. The RAST Server: Rapid annotations using subsystems technology. *BMC Genom.* **2008**, *9*, 75. [[CrossRef](#)]
53. Camacho, C.; Coulouris, G.; Avagyan, V.; Ma, N.; Papadopoulos, J.; Bealer, K.; Madden, T.L. BLAST+: Architecture and applications. *BMC Bioinform.* **2009**, *10*, 421. [[CrossRef](#)]
54. Meier-Kolthoff, J.P.; Goker, M. TYGS is an automated high-throughput platform for state-of-the-art genome-based taxonomy. *Nat. Commun.* **2019**, *10*, 2182. [[CrossRef](#)] [[PubMed](#)]
55. Kumar, S.; Stecher, G.; Li, M.; Nknyaz, C.; Tamura, K. MEGA X: Molecular Evolutionary Genetics Analysis across Computing Platforms. *Mol. Biol. Evol.* **2018**, *35*, 1547–1549. [[CrossRef](#)] [[PubMed](#)]
56. Lee, I.; Ouk Kim, Y.; Park, S.C.; Chun, J. OrthoANI: An improved algorithm and software for calculating average nucleotide identity. *Int. J. Syst. Evol. Microbiol.* **2016**, *66*, 1100–1103. [[CrossRef](#)] [[PubMed](#)]
57. Rodriguez-R, L.M.; Konstantinidis, K.T. The enveomics collection: A toolbox for specialized analyses of microbial genomes and metagenomes. *PeerJ* **2016**, *4*, e1900v1.
58. Medema, M.H.; Blin, K.; Cimermancic, P.; de Jager, V.; Zakrzewski, P.; Fischbach, M.A.; Weber, T.; Takano, E.; Breitling, R. antiSMASH: Rapid identification, annotation and analysis of secondary metabolite biosynthesis gene clusters in bacterial and fungal genome sequences. *Nucleic Acids Res.* **2011**, *39*, W339–W346. [[CrossRef](#)]
59. Blin, K.; Shaw, S.; Steinke, K.; Villebro, R.; Ziemert, N.; Lee, S.Y.; Medema, M.H.; Weber, T. antiSMASH 5.0: Updates to the secondary metabolite genome mining pipeline. *Nucleic Acids Res.* **2019**, *47*, W81–W87. [[CrossRef](#)] [[PubMed](#)]
60. Kautsar, S.A.; Blin, K.; Shaw, S.; Navarro-Munoz, J.C.; Terlouw, B.R.; van der Hooft, J.J.J.; van Santen, J.A.; Tracanna, V.; Suarez Duran, H.G.; Pascal Andreu, V.; et al. MIBiG 2.0: A repository for biosynthetic gene clusters of known function. *Nucleic Acids Res.* **2020**, *48*, D454–D458. [[CrossRef](#)]
61. Navarro-Munoz, J.C.; Selem-Mojica, N.; Mullowney, M.W.; Kautsar, S.A.; Tryon, J.H.; Parkinson, E.I.; De Los Santos, E.L.C.; Yeong, M.; Cruz-Morales, P.; Abubucker, S.; et al. A computational framework to explore large-scale biosynthetic diversity. *Nat. Chem. Biol.* **2020**, *16*, 60–68. [[CrossRef](#)]
62. Mistry, J.; Chuguransky, S.; Williams, L.; Qureshi, M.; Salazar, G.A.; Sonnhammer, E.L.L.; Tosatto, S.C.E.; Paladin, L.; Raj, S.; Richardson, L.J.; et al. Pfam: The protein families database in 2021. *Nucleic Acids Res.* **2021**, *49*, D412–D419. [[CrossRef](#)] [[PubMed](#)]
63. Shannon, P.; Markiel, A.; Ozier, O.; Baliga, N.S.; Wang, J.T.; Ramage, D.; Amin, N.; Schwikowski, B.; Ideker, T. Cytoscape: A software environment for integrated models of biomolecular interaction networks. *Genome Res.* **2003**, *13*, 2498–2504. [[CrossRef](#)] [[PubMed](#)]
64. Richter, M.; Rossello-Mora, R. Shifting the genomic gold standard for the prokaryotic species definition. *Proc. Natl. Acad. Sci. USA* **2009**, *106*, 19126–19131. [[CrossRef](#)] [[PubMed](#)]
65. Bentley, R.; Meganathan, R. Geosmin and methylisoborneol biosynthesis in streptomycetes. Evidence for an isoprenoid pathway and its absence in non-differentiating isolates. *FEBS Lett.* **1981**, *125*, 220–222. [[CrossRef](#)]

66. Dickschat, J.S.; Bode, H.B.; Mahmud, T.; Muller, R.; Schulz, S. A novel type of geosmin biosynthesis in myxobacteria. *J. Org. Chem.* **2005**, *70*, 5174–5182. [[CrossRef](#)]
67. Bhat, S.; Ahrendt, T.; Dauth, C.; Bode, H.B.; Shimkets, L.J. Two lipid signals guide fruiting body development of *Myxococcus xanthus*. *mBio* **2014**, *5*, e00939-13. [[CrossRef](#)]
68. Lorenzen, W.; Bozhuyuk, K.A.; Cortina, N.S.; Bode, H.B. A comprehensive insight into the lipid composition of *Myxococcus xanthus* by UPLC-ESI-MS. *J. Lipid Res.* **2014**, *55*, 2620–2633. [[CrossRef](#)]
69. Botella, J.A.; Murillo, F.J.; Ruiz-Vazquez, R. A cluster of structural and regulatory genes for light-induced carotenogenesis in *Myxococcus xanthus*. *Eur. J. Biochem.* **1995**, *233*, 238–248. [[CrossRef](#)]
70. Cervantes, M.; Murillo, F.J. Role for vitamin B(12) in light induction of gene expression in the bacterium *Myxococcus xanthus*. *J. Bacteriol.* **2002**, *184*, 2215–2224. [[CrossRef](#)]
71. Lopez-Rubio, J.J.; Elias-Arnanz, M.; Padmanabhan, S.; Murillo, F.J. A repressor-antirepressor pair links two loci controlling light-induced carotenogenesis in *Myxococcus xanthus*. *J. Biol. Chem.* **2002**, *277*, 7262–7270. [[CrossRef](#)]
72. Perez-Marin, M.C.; Padmanabhan, S.; Polanco, M.C.; Murillo, F.J.; Elias-Arnanz, M. Vitamin B12 partners the CarH repressor to downregulate a photoinducible promoter in *Myxococcus xanthus*. *Mol. Microbiol.* **2008**, *67*, 804–819. [[CrossRef](#)] [[PubMed](#)]
73. Gaitatzis, N.; Kunze, B.; Muller, R. In vitro reconstitution of the myxochelin biosynthetic machinery of *Stigmatella aurantiaca* Sg a15: Biochemical characterization of a reductive release mechanism from nonribosomal peptide synthetases. *Proc. Natl. Acad. Sci. USA* **2001**, *98*, 11136–11141. [[CrossRef](#)]
74. Li, Y.; Weissman, K.J.; Muller, R. Myxochelin biosynthesis: Direct evidence for two- and four-electron reduction of a carrier protein-bound thioester. *J. Am. Chem. Soc.* **2008**, *130*, 7554–7555. [[CrossRef](#)]
75. Cortina, N.S.; Krug, D.; Plaza, A.; Revermann, O.; Muller, R. Myxoprincomide: A natural product from *Myxococcus xanthus* discovered by comprehensive analysis of the secondary metabolome. *Angew. Chem. Int. Ed.* **2012**, *51*, 811–816. [[CrossRef](#)] [[PubMed](#)]
76. Sasse, F.; Steinmetz, H.; Hofle, G.; Reichenbach, H. Rhizopodin, a new compound from *Myxococcus stipitatus* (myxobacteria) causes formation of rhizopodia-like structures in animal cell cultures. Production, isolation, physico-chemical and biological properties. *J. Antibiot.* **1993**, *46*, 741–748. [[CrossRef](#)] [[PubMed](#)]
77. Pistorius, D.; Muller, R. Discovery of the rhizopodin biosynthetic gene cluster in *Stigmatella aurantiaca* Sg a15 by genome mining. *ChemBiochem* **2012**, *13*, 416–426. [[CrossRef](#)]
78. Park, S.; Hyun, H.; Lee, J.S.; Cho, K. Identification of the Phenalamide Biosynthetic Gene Cluster in *Myxococcus stipitatus* DSM 14675. *J. Microbiol. Biotechnol.* **2016**, *26*, 1636–1642. [[CrossRef](#)]
79. Blin, K.; Shaw, S.; Kautsar, S.A.; Medema, M.H.; Weber, T. The antiSMASH database version 3: Increased taxonomic coverage and new query features for modular enzymes. *Nucleic Acids Res.* **2021**, *49*, D639–D643. [[CrossRef](#)]
80. Meiser, P.; Weissman, K.J.; Bode, H.B.; Krug, D.; Dickschat, J.S.; Sandmann, A.; Muller, R. DKxanthene biosynthesis—understanding the basis for diversity-oriented synthesis in myxobacterial secondary metabolism. *Chem. Biol.* **2008**, *15*, 771–781. [[CrossRef](#)] [[PubMed](#)]
81. Panter, F.; Krug, D.; Muller, R. Novel Methoxymethacrylate Natural Products Uncovered by Statistics-Based Mining of the *Myxococcus fulvus* Secondary Metabolome. *ACS Chem. Biol.* **2019**, *14*, 88–98. [[CrossRef](#)] [[PubMed](#)]
82. Momen, A.Z.; Hoshino, T. Biosynthesis of violacein: Intact incorporation of the tryptophan molecule on the oxindole side, with intramolecular rearrangement of the indole ring on the 5-hydroxyindole side. *Biosci. Biotechnol. Biochem.* **2000**, *64*, 539–549. [[CrossRef](#)]
83. Brady, S.F.; Chao, C.J.; Handelsman, J.; Clardy, J. Cloning and heterologous expression of a natural product biosynthetic gene cluster from eDNA. *Org. Lett.* **2001**, *3*, 1981–1984. [[CrossRef](#)] [[PubMed](#)]
84. Hoshino, T. Violacein and related tryptophan metabolites produced by *Chromobacterium violaceum*: Biosynthetic mechanism and pathway for construction of violacein core. *Appl. Microbiol. Biotechnol.* **2011**, *91*, 1463–1475. [[CrossRef](#)]
85. Erol, O.; Schaberle, T.F.; Schmitz, A.; Rachid, S.; Gurgui, C.; El Omari, M.; Lohr, F.; Kehraus, S.; Piel, J.; Muller, R.; et al. Biosynthesis of the myxobacterial antibiotic coralopyronin A. *ChemBiochem* **2010**, *11*, 1253–1265. [[CrossRef](#)] [[PubMed](#)]
86. Pogorevc, D.; Panter, F.; Schillinger, C.; Jansen, R.; Wenzel, S.C.; Muller, R. Production optimization and biosynthesis revision of coralopyronin A, a potent anti-filarial antibiotic. *Metab. Eng.* **2019**, *55*, 201–211. [[CrossRef](#)]
87. Weinig, S.; Hecht, H.J.; Mahmud, T.; Muller, R. Melithiazol biosynthesis: Further insights into myxobacterial PKS/NRPS systems and evidence for a new subclass of methyl transferases. *Chem. Biol.* **2003**, *10*, 939–952. [[CrossRef](#)]
88. Schieferdecker, S.; Konig, S.; Weigel, C.; Dahse, H.M.; Werz, O.; Nett, M. Structure and biosynthetic assembly of gulfmirecins, macrolide antibiotics from the predatory bacterium *Pyxidicoccus fallax*. *Chemistry* **2014**, *20*, 15933–15940. [[CrossRef](#)] [[PubMed](#)]
89. Surup, F.; Viehrig, K.; Mohr, K.I.; Herrmann, J.; Jansen, R.; Muller, R. Disciformycins A and B: 12-membered macrolide glycoside antibiotics from the myxobacterium *Pyxidicoccus fallax* active against multiresistant staphylococci. *Angew. Chem. Int. Ed.* **2014**, *53*, 13588–13591. [[CrossRef](#)]
90. Panter, F.; Krug, D.; Baumann, S.; Muller, R. Self-resistance guided genome mining uncovers new topoisomerase inhibitors from myxobacteria. *Chem. Sci.* **2018**, *9*, 4898–4908. [[CrossRef](#)] [[PubMed](#)]
91. Gregory, K.; Salvador, L.A.; Akbar, S.; Adaihpoh, B.I.; Stevens, D.C. Survey of Biosynthetic Gene Clusters from Sequenced Myxobacteria Reveals Unexplored Biosynthetic Potential. *Microorganisms* **2019**, *7*, 781. [[CrossRef](#)] [[PubMed](#)]